Microstructure and Electrical Resistivity of Low-Temperature-Cured Silver Films Prepared Using Silver Oxide and Silver Stearate Pastes

2009 Jpn. J. Appl. Phys. 48 016501

(http://iopscience.iop.org/1347-4065/48/1R/016501)

Microstructure and Electrical Resistivity of Low-Temperature-Cured Silver Films Prepared Using Silver Oxide and Silver Stearate Pastes

Hong-Ching Lin, Pang Lin, Chun-An Lu[1], and Sea-Fue Wang[2*]

Department of Materials Science Engineering, National Chiao Tung University, Hsinchu, Taiwan 300, R.O.C.
[1]*Material and Chemical Research Laboratories, Industrial Technology Research Institute, Hsinchu, Taiwan 310, R.O.C*
[2]*Department of Materials and Mineral Resources Engineering, National Taipei University of Technology, Taipei, Taiwan 106, R.O.C.*

Received April 2, 2008; revised May 3, 2008; accepted May 7, 2008; published online January 20, 2009

In this study, paste formulations containing silver oxide coated with a metallo-organic decomposition (MOD) agent of silver stearate were prepared without using any silver powders or silver flakes. Results indicate that all pastes appear to have a pseudoplastic flow property that is acceptable for roll-to-roll printing and screen printing. The pastes were screen-printed on an alumina substrate and then thermally treated in a range of temperatures. The lowest electrical resistivity of 13.2×10^{-6} Ω·cm was obtained for the film prepared from paste with a Ag_2O/silver stearate ratio of 100 : 5 at a solid loading of 80 wt % in the solvent α-terpineol, after being cured at 160 °C for 5 min, which meets the requirements of low-temperature and high-speed manufacturing for practical applications. The low resistivity of the film is facilitated by the combination of Ag_2O and silver stearate added to the paste. Ag_2O produces a high density of silver matrix after being reduced at low temperatures, and the presence of silver stearate contributes to the rheological behavior of the paste after dissolution in the solvent. Coexistence of Ag_2O and silver stearate induces their simultaneous transformation to the silver form at temperatures below 160 °C.

DOI: 10.1143/JJAP.48.016501

1. Introduction

Flexible electronics is emerging as a multidisciplinary research topic with far-reaching impact on a number of research areas, including flat-panel displays, organic electronics and distributed macroelectronic systems and architectures. To develop flexible electronics, each component must be amenable to a low-temperature process, adhesion to polymer-based substrates, and low-cost and high-speed manufacturing, and has high performance. Screen printing, electrophotographic printing, and ink-jet printing have been used to form precise electrically conductive patterns by depositing metal particles onto an insulating substrate surface. In particular, screen printing and ink-jet printing have been used for printing antennas in radio frequency identification (RFID) tags.[1)]

Most commercial conductive pastes designed for various printing processes are formulated using the conducting metal particles dispersed in a resin or a solvent. The conductive pastes are mainly classified into two types, namely, the firing-type conductive paste and resin-type conductive paste. The former has glass as the binder, which forms into a conductive film when heated at temperatures ranging from 500 to 900 °C. The latter contains a resin as the binder and vehicle, which requires only a low-temperature curing process to form a continuous film. However, glasses and resins are generally nonconductive, which may hinder the contacts of metal powders and reduce electron transmission. Recently, there has been a tremendous interest in low-curing-temperature conductive pastes, which have no glass or resin added, but manufactured at a low cost and high speed for flexible electronic applications.

Conventional low-curing-temperature pastes have several limitations, such as relatively low electrical conductivity and unstable contact resistance. Several approaches were proposed to overcome these obstacles. The first is the use of a suspension of metal nanoparticles. The small size of nanoparticles results in a melting point considerably lower than their bulk-material counterparts.[2)] After a printing process, the metallic nanoparticles can subsequently be sintered at a plastic-compatible temperature. The second is the use of metals with a lower melting point that form interconnections between metal particles. Another approach is the use of metallo-organic decomposition (MOD) technology. High-conductivity metal films can be achieved at a low temperature by decomposing metallo-organic precursors on various substrates, where the molecular nature of the compounds allows a low-temperature conversion to metal. Teng and Vest employed MOD inks to metallization of solar cells.[4)] They successfully applied an ink-jet printing system with silver neodecanoate MOD ink to hybrid microcircuits.[5)] Lu *et al.* utilized a silver paste comprising silver flakes, inorganic salt of silver oxalate ($Ag_2C_2O_4$), and organic acidic salt of silver 2-ethylhexanoate ($C_8H_{15}O_2Ag$) for forming a conductive film on the substrate at a relatively low temperature.[3,6)] The MOD-metal flake mixture maintains its configuration during heating, and will decompose to form a well-bonded, well-resolved conductor at a temperature compatible to polymer-based circuit board substrates. The electrical conductivity is equal to that obtained using conventional thick film conductors sintered at high temperatures (>700 °C).

High-density and high-conductivity metal layers can also be obtained at a low temperature by thermal reduction of silver oxide using various reducing agents.[7)] Silver oxide has been studied extensively for its applications in electrical, optical, and magneto-optical data storage industries.[8,9)] A previous study[13)] indicated that MOD silver pastes with partial substitution of silver flake by Ag_2O and AgO enhance the connectivity and packing density of the silver flakes, and thus increases the electrical conductivity of the films. A resistivity of 14×10^{-6} Ω·cm was achieved for the MOD paste with 20 wt % Ag_2O added after being cured at 200 °C for 5 min. However, for the flexible PET substrate, the curing of pastes has to proceed at temperatures not higher than 170 °C, and the resultant film has to possess a low electrical resistivity.[14)] Also, our previous study[15)] showed that silver stearate, a salt derived from stearic acid, can

*E-mail address: sfwang@ntut.edu.tw

easily wet silver flake powders and distribute itself uniformly between the metal or oxide powders. In this study, paste formulations containing silver oxide coated with various amounts of MOD silver stearate [$Ag(O_2C(CH_2)_{16}CH_3)$] were prepared without using silver powders or silver flakes. The prepared pastes were screen-printed on an alumina substrate and then thermally treated in a range of temperatures. The microstructures and electrical properties of resultant films were characterized and discussed.

2. Experiments

The low-curing-temperature silver pastes used in this study were prepared from commercially available silver(I) oxide (99.99%, American Elements), the MOD compound silver stearate [$Ag(O_2C(CH_2)_{16}CH_3)$; GROTTO], and the solvent α-terpineol (TCI). Ag_2O powders have an average particle size (d_{50}) of 2.35 μm, measured by light scattering (Horiba LA-910). First, Ag_2O and silver stearate were mixed at different weight ratios (100 : 3; 100 : 4; 100 : 5; and 100 : 6) by dry ball-milling for 24 h. Then the silver-stearate-coated silver oxide powders were mixed with solvent α-terpineol using a high-speed mixer (Thinky Mixer) for 3 min and debubbled for 1 min. The weight ratios of silver-stearate-coated Ag_2O powders to the solvent was fixed at 70, 75, and 80 wt %. The formulations of low-curing-temperature silver pastes prepared in this study are listed in Table I.

To understand the thermal behavior, the thermogravimetric analysis (TGA; Perkin-Elmer) of various amounts of silver-stearate-coated Ag_2O powders and the paste samples of different solid loadings were performed in air at a heating rate of 10 °C/min. X-ray diffraction (XRD; Rigaku DMX-2200) analysis using monochromated Cu Kα radiation was performed for the phase identification of the films after heat treatment. Rheological behaviors of the pastes with solid contents of 70, 75, and 80 wt % were explored using a HBT model viscometer (Brookfield DV-II) using a "40" spindle.

Silver metal lines with a length (l) of 10 cm, a line width (w) of 2–4 mm, and a line thickness (d) of 20–40 μm were manually printed on the alumina substrate for resistivity measurement. A Keithley 2400 multimeter with a four-point probe was used to measure the bulk resistance of cured silver paste. The resistivity (ρ) of the silver conducting line cured at various temperatures was calculated using the relationship $\rho = (R \cdot w \cdot d)/l$, in which R is the resistance of the line. α-step was used to measure the line morphology with line width (w) and line thickness (d). The microstructures of pure Ag_2O powder, coated powders, and films cured at various thermal profiles were investigated by field-emission scanning electron microscopy (SEM; Hitachi S4500) and transmission electron microscopy (TEM; Philips Tecnai F20).

3. Results and Discussion

The thermal decomposition behaviors of mixtures containing α-terpineol, Ag_2O, or silver stearate characterized by TGA are shown in Fig. 1. For the mixture of 70 wt % α-terpineol and 30 wt % Ag_2O, a significant weight loss was observed below 189 °C and then the sample weight loss levels off at 28.3 wt % of its original weight, which is close to the theoretical weight percentage determined taking into account the evaporation of α-terpineol and the reduction of Ag_2O to silver. It appears that Ag_2O can catalyze the decomposition of the α-terpenol solvent, which is identical to the results of a previous study.[13] For the TGA traces of 70 wt % α-terpineol and 30 wt % silver stearate, there are three regions with significant weight loss, including ≈70 wt % weight loss below 198 °C owing to the evaporation of α-terpineol and then a complete ≈22 wt % weight loss in the temperature range from 198 to 380 °C resulting from the thermal decomposition of silver stearate. Above 380 °C, there is no further weight loss, which reveals that all silver compounds were transformed into silver. For the mixture of 70 wt % α-terpineol, 20 wt % Ag_2O, and 10 wt % silver stearate, ≈72.2 wt % weight loss was observed below 189 °C, which corresponds to the combination of the evaporation of 70 wt % α-terpineol, the reduction of 20 wt % Ag_2O, and the decomposition of 1.1 wt % silver stearate. The remaining 8.9 wt % silver stearate was further decomposed at temperatures above ≈240 °C. No weight loss was observed at temperatures higher than 260 °C. Appa-

Table I. Formulations of low-curing-temperature silver pastes prepared in this study.

Solid loading (wt %)	Weight ratio of Ag_2O to silver stearate	Paste composition (wt %)			Total Ag content in paste (wt %)
		Ag_2O	Silver stearate	α-Terpineol	
70	100 : 3	67.96	2.04	30	63.83
	100 : 4	67.31	2.69	30	63.41
	100 : 5	66.67	3.33	30	62.99
	100 : 6	66.04	3.96	30	62.57
75	100 : 3	72.82	2.18	25	68.40
	100 : 4	72.12	2.88	25	67.94
	100 : 5	71.43	3.57	25	67.48
	100 : 6	70.75	4.25	25	67.04
80	100 : 3	77.67	2.33	20	72.95
	100 : 4	76.92	3.08	20	72.46
	100 : 5	76.19	3.81	20	71.98
	100 : 6	75.47	4.53	20	71.51

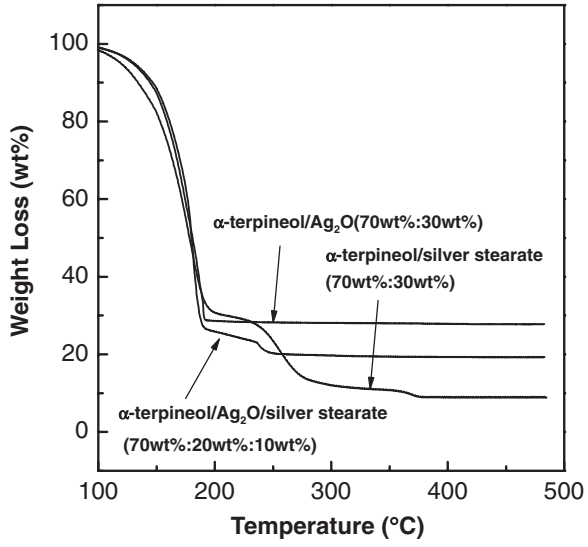

Fig. 1. TGA results of pastes prepared at various Ag_2O/silver stearate ratios (100 : 3, 100 : 4, 100 : 5, and 100 : 6).

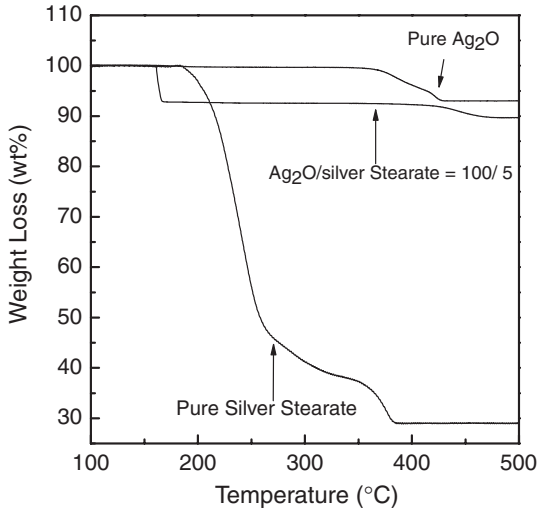

Fig. 2. TGA results of pure silver oxide, pure silver stearate, and mixture of Ag_2O and silver stearate (100 : 5).

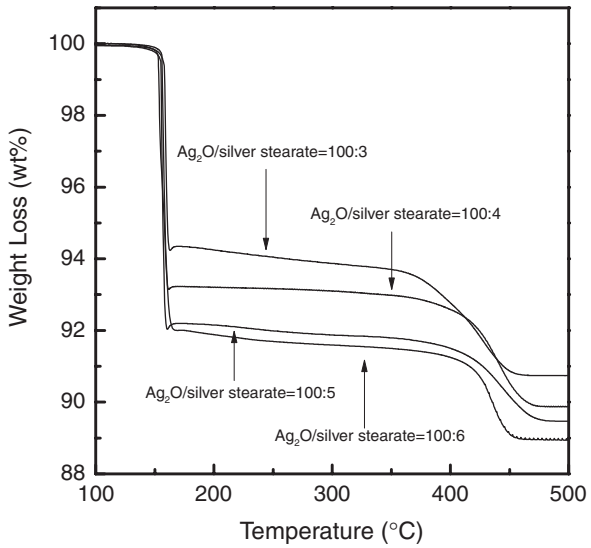

Fig. 3. TGA results of mixtures of Ag_2O and silver stearate at various ratios.

rently, Ag_2O can catalyze the decomposition of silver stearate, including 1.1 wt % below 189 °C and the rest between 189 and 260 °C. Calculations based on the above results indicate that 100 g of Ag_2O can catalyze the decomposition of ≈5.5 g silver stearate at temperatures below 189 °C; however, the weight ratio for the reaction between Ag_2O and silver stearate is dependent on the physical characteristics of Ag_2O powders, such as particle size.

Figure 2 shows the TGA traces of Ag_2O, silver stearate, and Ag_2O with 5 wt % silver stearate. Without α-terpineol, Ag_2O is not reduced until the temperature reaches 370 °C. The thermal decomposition path of pure silver stearate is similar to that observed in the mixture of α-terpineol and silver stearate, as shown in Fig. 1. It is evident that α-terpineol promotes the reduction of Ag_2O but not the decomposition reaction of silver stearate. For Ag_2O with 5 wt % silver stearate, a rapid ≈7.8 wt % weight loss was observed at ≈160 °C, which corresponds to the transformation of silver compounds into pure silver (89.9% of the original weight theoretically). XRD analysis of the sample heat-treated at 160 °C indicates that silver and a small amount of Ag_2O are present in the residue. It shows that Ag_2O catalyzes the decomposition of silver stearate and the decomposed silver induces the reduction of Ag_2O concurrently, which confirms the observation shown in Fig. 1. Not all of Ag_2O was reduced to silver. The Ag_2O residue was transferred back to silver at temperatures higher than 410 °C, which is in agreement with the observation reported in the literature.

In order to determine the optimum ratio of Ag_2O/silver stearate, TGA studies of silver oxide with additions of 3, 4, 5, and 6 wt % silver stearate were performed and the results are shown in Fig. 3. Similar to the decomposition behavior of Ag_2O/silver stearate shown in Fig. 2, the mixtures showed marked decreases in weight at temperatures ranging from 155 to 160 °C, and Ag_2O residues were reduced back to silver at temperatures higher than 410 °C. Increasing the amount of silver stearate added increases the weight loss due to the complete decomposition of silver stearate and partial reduction of Ag_2O. As more fresh silver decomposed from silver stearate, more Ag_2O was catalyzed and reduced back to silver. Comparing the weight loss at 165 °C for samples with 5 and 6% stearate, the ≈0.2 wt % difference in weight loss observed corresponds to the decomposition of silver stearate. No additional reduction of Ag_2O was observed. Therefore, it can be concluded that for a silver stearate content exceeding 5 wt %, the weight loss at temperatures below 160 °C corresponding to the reduction of Ag_2O does not increase.

In this study, the silver flake and binder such as ethyl cellulose were replaced by Ag_2O and silver stearate in the paste, to decrease curing temperature while maintaining the required paste characteristics and electrical properties of the final film. Rheological behaviors of the pastes with solid loadings of 70 and 80 wt % are characterized and the results are shown in Figs. 4(a) and 4(b), respectively. It was elucidated by calculating shear stress versus shear rate at various ratios of Ag_2O and silver stearate. The results indicate that all pastes appear to have the pseudoplastic flow (shear-thinning) property. The initial shear stress and viscosity increase with increasing silver stearate content and solid loading. The dissolution of silver stearate in solvent increased the viscosity of the paste significantly. It is similar to that observed in conventional isotropically conductive adhesive (ICA) formulations, in which stearic acids are widely used as the rheology modification agent or lubricant layer on the surfaces of metal powders, to modify the viscosity of conductive adhesive paste.[16] For the paste with 80 wt % solid loading, the pastes with 5 and 6 wt % silver stearate show shear-thinning with an apparent yield point. The dissolution of silver steatrate in solvent leads to viscoelasticity properties with a stable viscosity and shear stress versus shear rate, which is acceptable for high shear rate applications, such as roll-to-roll printing and screen printing.[3]

Figures 5(a) and 5(b) show the electrical resistivities of silver films prepared from the pastes with solid loadings of 70, 75, and 80 wt %, after curing at 160 °C for 5 and 10 min,

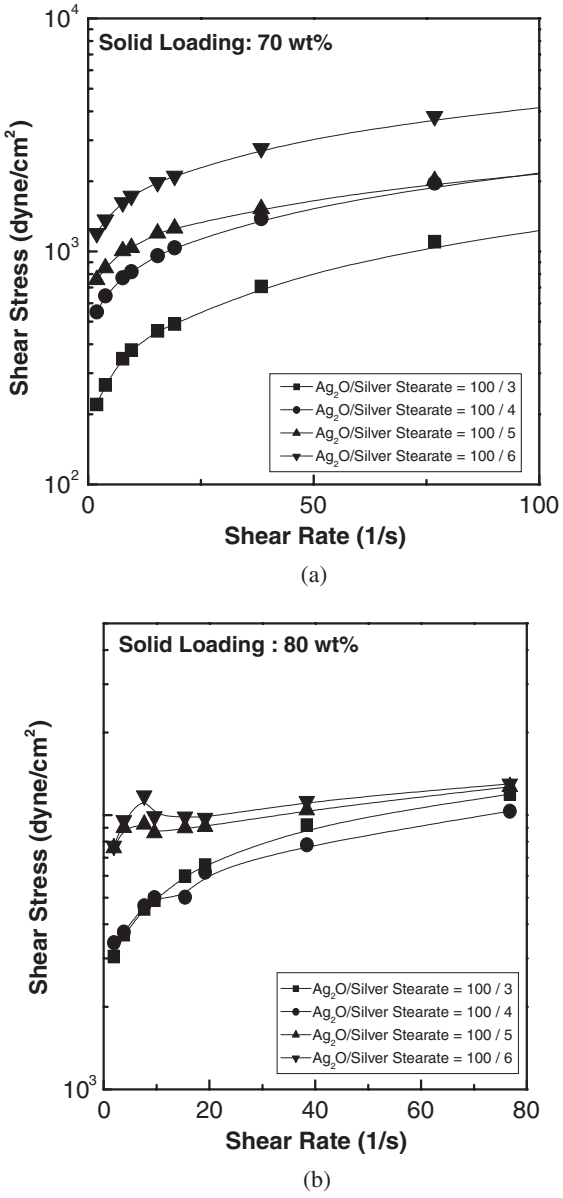

Fig. 4. Rheological behaviors of pastes with various ratios of Ag_2O and silver stearate at solid loadings of (a) 70 and (b) 80 wt %.

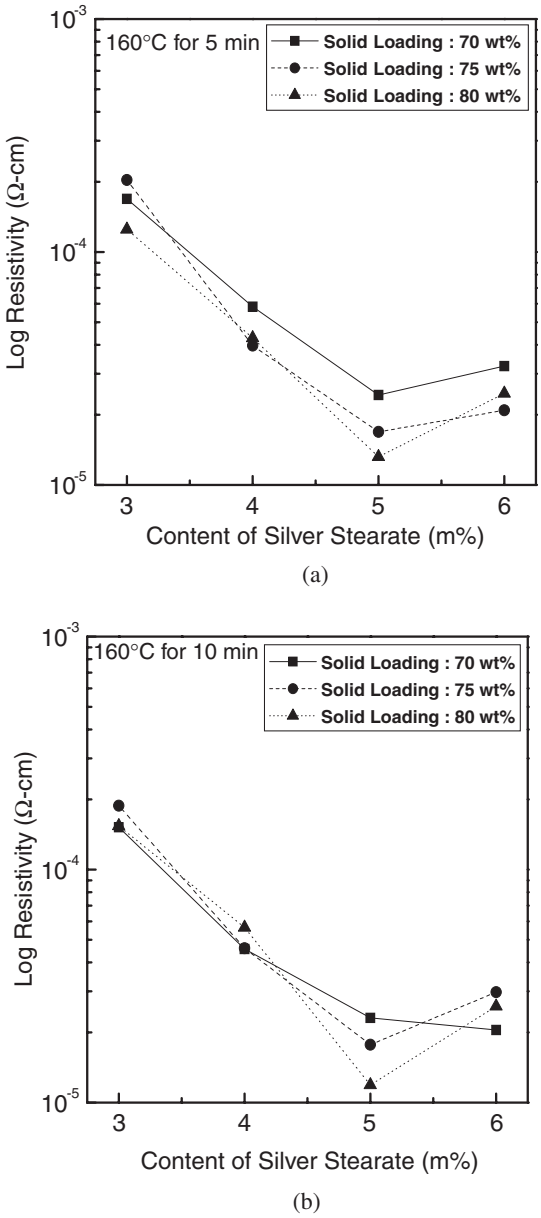

Fig. 5. Electrical resistivities of silver films prepared from pastes with various Ag_2O/silver stearate ratios and solid loadings, after curing at 160 °C for (a) 5 and (b) 10 min.

respectively. The film resistivity decreases with increasing ratio of Ag_2O/silver stearate up to 100 : 5 and then increases again with the content of silver stearate. Increasing the soaking time from 5 to 10 min does not change the resistivity significantly. Electrical resistivity decreases with solid loading, which is due to the higher packing density of conducting particles after curing. The electrical resistivity of the films prepared from pastes with a Ag_2O/silver stearate ratio of 100 : 5, at solid loadings of 70, 75, and 80 wt % are 24.3×10^{-6}, 16.9×10^{-6}, and $13.2 \times 10^{-6}\,\Omega$·cm, respectively, after curing at 160 °C for 5 min, which meets the requirements of low-temperature and high-speed manufacturing for practical applications. The electrical resistivity of the film depends on the connectivity and film density of various species in the film. As the paste is heated, Ag_2O catalyzes the decomposition of silver stearate and, simultaneously, undergoes reduction and transformation to silver particles, which may be catalyzed by the fresh fine silver particles formed on their surfaces. Reduction of Ag_2O and thermal decomposition of silver stearate proceed with time during curing, which decreases the resivitivity of the films. Residual Ag_2O was found by XRD analysis of the films after curing at 160 °C, as shown in Fig. 6. It is sufficiently clear that the reduction reaction of Ag_2O does not proceed to completion, and leads to a small quantity of Ag_2O still remaining after thermal curing. The incomplete reduction reaction of Ag_2O retards a further decrease in the resistivity of silver films.

Ag_2O catalyzes the evaporation of α-terpineol and the decomposition of silver stearate, which decreases the curing temperature of films to 160 °C and shortens the soaking time to 5 min. At a lower content of silver stearate (Ag_2O/silver stearate = 100 : 3), the insufficient amount of fine silver particles decomposed from silver stearate leads to a higher resistivity. At a higher content of silver stearate (Ag_2O/silver stearate = 100 : 6), the extra silver stearate

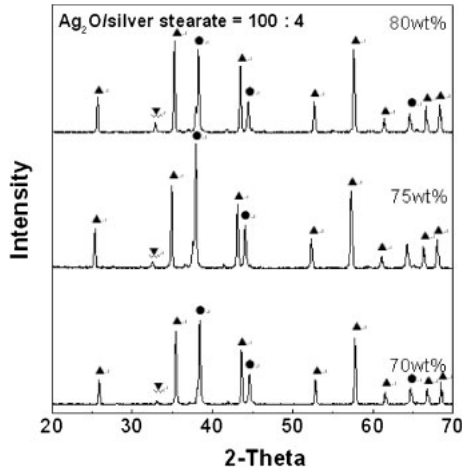

Fig. 6. XRD analysis results of film with Ag_2O/silver stearate ratio of 100 : 4, after curing at 160 °C for 10 min.

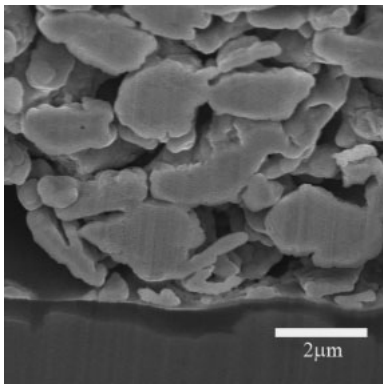

Fig. 8. SEM cross-sectional images of film, prepared from paste with Ag_2O/silver stearate ratio of 100 : 5 at solid loading of 80 wt % and after curing at 160 °C for 10 min.

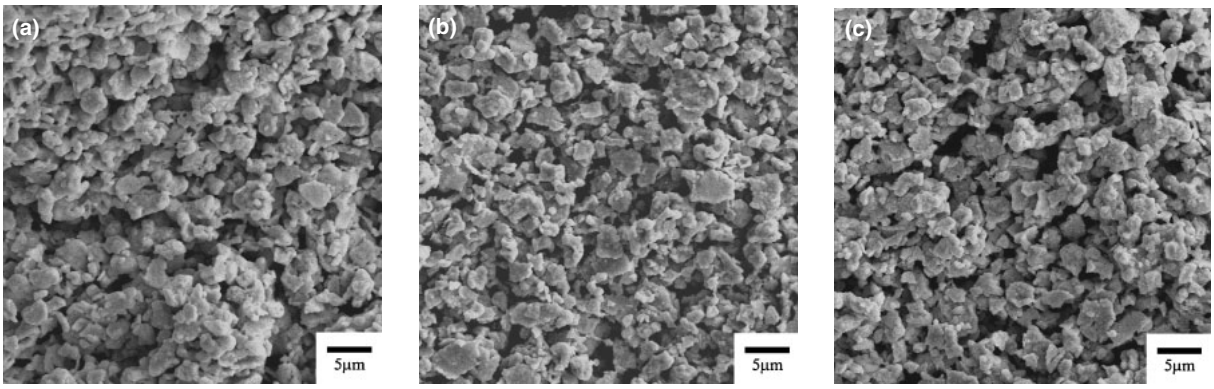

Fig. 7. SEM images of films, prepared from pastes with Ag_2O/silver stearate ratios of (a) 100 : 4, (b) 100 : 5, and (c) 100 : 6, at solid loading of 80 wt % and after curing at 160 °C for 10 min.

could not further induce the reduction of Ag_2O during curing and, also, the high viscosity of the paste owing to the dissolution of silver stearate in the solvent decreases packing density (Figs. 4 and 5). Therefore, a higher electrical resistivity was obtained at Ag_2O/silver stearate ratios of 100 : 3 and 100 : 6 after curing.

SEM images of the films, prepared from the pastes with various Ag_2O/silver stearate ratios at a solid loading of 80 wt %, after curing at 160 °C for 10 min are shown in Fig. 7. They indicate that the linkage of silver particles from the thermal decomposition of silver stearate and the reduction of Ag_2O results in a high electrical conductivity of films after curing. For a Ag_2O/silver stearate ratio of 100/5, the microstructure seems to have the highest film density, which is coincident with the lowest electrical resistivity of films shown in Fig. 5. A SEM cross-sectional image of the films shown in Fig. 8 shows the interconnection of silver grains that contributes to the low electrical resistivity. Upon careful examination of the microstructure of the films, it appears that the three-dimensional interconnection network has resulted from the coalescence of fine and fresh silver particles decomposed from silver stearate and the neckgrowth of coarse silver grains reduced from Ag_2O. A TEM image (Fig. 9) shows silver nano particles coated on the surfaces of silver grains, which were reduced

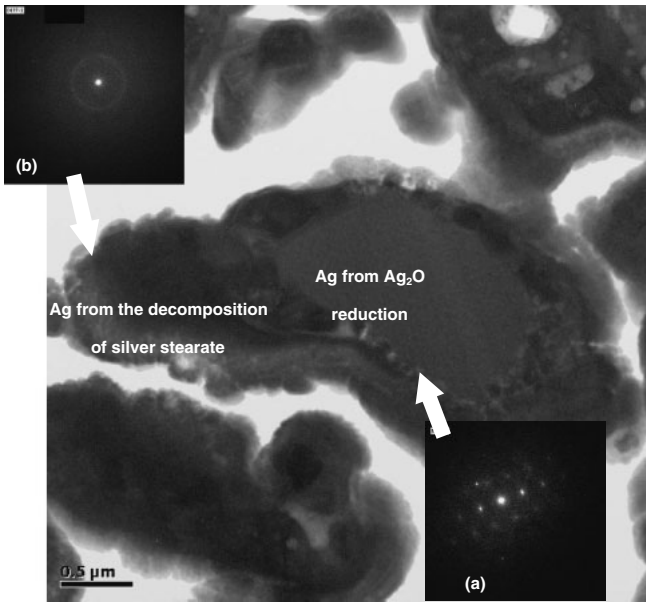

Fig. 9. TEM image of microstructure of film prepared from pastes with Ag_2O/silver stearate ratio of 100 : 3, at solid loading of 80 wt % and after curing at 160 °C for 10 min.

from Ag_2O. The left-top (a) diffraction pattern corresponds to the silver produced from the reduction of Ag_2O and the right-down ring diffraction pattern is due to the silver produced from the decomposition of silver stearate. Small silver particles are formed from decomposition of silver stearate catalyzed by Ag_2O, which then adher onto the surfaces of silver grains that are also simultaneously reduced from Ag_2O. Neckgrowth and sintering of silver particles shown in the TEM image illustrate the low electrical resistivity of films after curing. The low resistivity of the films is facilitated by the combination of Ag_2O and silver stearate contained in the paste used. Ag_2O consists of a high silver constituent (100 g of Ag_2O produces 93.1 g of silver), which produces a high density of a silver matrix after reduction at low temperatures. The presence of a small amount of silver stearate contributes to the rheological behavior of the paste owing to its dissolution in the solvent. More importantly, the coexistence of Ag_2O and silver stearate induces their transformation into the silver form simultaneously at temperatures below 160 °C.

4. Conclusions

In this study, the silver flake and binder in the paste were replaced by Ag_2O and silver stearate, to decrease the curing temperature while maintaining the required paste characteristics and electrical properties of the final film. Results indicate that all pastes appear to have the pseudoplastic flow (shear-thinning) property. The initial shear stress and viscosity increases with increasing silver stearate content and solid loading. As the paste is heated, Ag_2O catalyzes the decomposition of silver stearate and, simultaneously, undergoes reduction and transformation into silver particles. The lowest electrical resistivity of $13.2 \times 10^{-6}\,\Omega\cdot$cm was obtained for the film prepared from paste with a Ag_2O/silver stearate ratio of 100 : 5 at a solid loading of 80 wt % in solvent α-terpineol, after curing at 160 °C for 5 min. The three-dimensional interconnection network resulted from the coalescence of fine silver particles decomposed from silver stearate and the neckgrowth of the coarse silver grains reduced from Ag_2O. Ag_2O catalyzes the evaporation of α-terpineol and the decomposition of silver stearate, which decreases the curing temperature of films to 160 °C and shortens the soaking time to 5 min.

1) D. Redinger, S. Yin, R. Farschi, and V. Subramanian: IEEE. Trans. Electron Devices **51** (2004) 1978.
2) V. Subramanian, P. C. Chang, J. B. Lee, A. R. Murphy, D. R. Redinger, and S. K. Volkman: Proc. IEEE **93** (2005) 1330.
3) C. A. Lu, P. Lin, H. C. Lin, and S. F. Wang: Jpn. J. Appl. Phys. **46** (2007) 251.
4) K. F. Teng and R. W. Vest: IEEE. Trans. Components Hybrids Manuf. Technol. **11** (1988) 291.
5) K. F. Teng and R. W. Vest: IEEE. Trans. Components Hybrids Manuf. Technol. **10** (1987) 545.
6) C. A. Lu, P. Lin, H. C. Lin, and S. F. Wang: submitted to Microelectron. Eng. (2007).
7) T. Honda: U.S. Patent 20040248998 A1 (2004).
8) J. Passaniti and S. A. Megahed: in *Handbook of Batteries*, ed. D. Linden (McGraw-Hill, New York, 1995) 2nd ed., p. 122.
9) D. F. Smith, G. R. Graybill, R. K. Grubbs, and J. A. Gucinski: J. Power Sources **65** (1997) 47.
10) *Thermal Properties of Inorganic Substances*, ed. K. Hesselmann (Springer, New York, 1991) p. 11.
11) B. V. L'vov: Thermochim. Acta **333** (1999) 13.
12) W. A. Parkhurst, S. Dallek, and B. F. Larrick: J. Electrochem. Soc. **131** (1984) 1739.
13) C. A. Lu, P. Lin, H. C. Lin, and S. F. Wang: Jpn. J. Appl. Phys. **46** (2007) 4179.
14) D. Huang, F. Liao, S. Molesa, D. Redinger, and V. Subramanian: J. Electrochem. Soc. **150** (2003) G412.
15) C. A. Lu, P. Lin, H. C. Lin, and S. F. Wang: Jpn. J. Appl. Phys. **45** (2006) 6987.
16) D. Lu and C. P. Wang: J. Therm. Anal. Calorimetry **61** (2000) 3.